Available online at www.sciencedirect.com

ScienceDirect

journal homepage: www.elsevier.com/locate/he

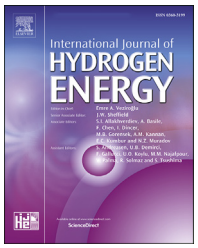

Application of similarity theory in modeling the output characteristics of proton exchange membrane fuel cell

Fan Bai [a], *Le Lei* [a], *Zhuo Zhang* [a], *Hailong Li* [b], *Jinyue Yan* [b], *Li Chen* [a], *Yan-Jun Dai* [a], *Lei Chen* [a], *Wen-Quan Tao* [a,*]

[a] *Key Laboratory of Thermo-Fluid Science & Engineering of MOE Xi'an Jiaotong University, Xi'an, Shaanxi, 710049, PR China*

[b] *School of Sustainable Development of Society and Technology, Malardalen University, SE 721 23, Västrås, Sweden*

HIGHLIGHTS

- Seven criteria composed of PEMFC input parameters are derived.
- Dimensionless voltage and electrical current are defined and calculated.
- The correctness and application prospect of the derived criteria are presented.
- Sensibilities of seven similarity criteria on the polarization curve are analyzed.

ARTICLE INFO

Article history:
Received 11 April 2021
Received in revised form
3 August 2021
Accepted 27 August 2021
Available online 17 September 2021

Keywords:
Proton exchange membrane fuel cell
Similarity analysis
Dimensionless polarization curve
Sensibility analysis

ABSTRACT

Proton Exchange Membrane Fuel Cell (PEMFC) has attracted widespread interest. In the present work, similarity analysis is adopted for a three-dimensional single-phase isothermal model of PEMFC to derive similarity criteria. Seven kinds of input criteria (Π_1 ~ Π_7) are obtained, relevant to the fluid flow, pressure drop, flow resistance in a porous medium, activity loss, diffusion mass transfer, convective mass transfer and ohmic loss in PEMFC respectively. Dimensionless voltage and dimensionless current density are defined as two output criteria. Numerical verifications show that if the seven criteria keep their individual values with their components vary in a wide range, the dimensionless polarization curves keep the same with a deviation about 1%, showing the validity and feasibility of the present analysis. From the effect on the dimensionless polarization curve, sensibility analysis shows that the seven criteria can be divided into three categories: strong (Π_4 and Π_7, -94.9% ~ +349.2%), mild to minor (Π_5 and Π_6, -4.5% ~ +5.0%), and negligible (Π_1, Π_2 and Π_3, -1.2% ~ +1.1%). The similarity analysis approach can greatly save computation time in modeling the output characteristics of PEMFC.

* *Corresponding author.*
E-mail addresses: baifan008aq@qq.com (F. Bai), leile2015@stu.xjtu.edu.cn (L. Lei), jczzzz@stu.xjtu.edu.cn (Z. Zhang), hailong.li@mdh.se (H. Li), jinyue@kth.se (J. Yan), lichennht08@mail.xjtu.edu.cn (L. Chen), daiyanjun2015@xjtu.edu.cn (Y.-J. Dai), chenlei@mail.xjtu.edu.cn (L. Chen), wqtao@mail.xjtu.edu.cn (W.-Q. Tao).

https://doi.org/10.1016/j.ijhydene.2021.08.205
0360-3199/

List of symbols and abbreviations*

Symbols

C	Proportionality coefficient
$\bar{J}_{cell}$	Dimensionless current density
l	Length, [m]
$\overline{V}_{cell}$	Dimensionless voltage
η	Overpotential, [V]
μ	Viscosity, [Pa·s]
μ_r	Relative viscosity, viscosity of flow in a porous medium compare with that without a porous medium
Π	Dimensionless number obtained by similarity analysis
ϕ_s	Electrical potential, [V]
ϕ_m	Ionic potential, [V]

Acronym

A	Anode
BP	Bipolar plate
C	Cathode
CH	Gas flow channel
CL	Catalyst layer
GDL	Gas diffusion layer
MEM	Membrane
PEMFC	Proton exchange membrane fuel cell

Introduction

Along with the coming hydrogen energy era, proton exchange membrane fuel cell (PEMFC) will become one of the most widespread power generating facilities which may serve as a substitute to diesel engines and even gasoline engines. In the last decade, PEMFC has received extensive attention and developed very fast. According to the statistics in Ref. [1], about 1800 articles on PEMFCs and about 10,000 papers on fuel cells were published each year.

As proposed by Ticianelli et al., in 1988 [2,3], polarization curve has been adopted in most of the related studies to describe the output characteristics of a fuel cell. PEMFC is a complex multi-phase multi-physics multi-scale coupled system [4] with a sandwich structure constituted by 9 layers [5], as shown in Fig. 1. Polarization curve of PEMFC is determined by dozens of parameters, including structure, physical, chemical and working parameters [6–8]. Previous studies have proposed several physical models [6,7,9–14] to numerically predict the output characteristics and field distribution of PEMFC [15–20]. Usually such models contain a great quantity of parameters whose number is often much larger than 20. One dimensional polarization curve can only represent the result of one combination of such parameters. In order to reveal the effects of different parameters on the polarization curve, many studies have been conducted, including parameter sensitivity analyses [21–24]. However, a complete understanding of the effects of different parameters on performance of PEMFCs is very difficult to obtain. One of the important reasons comes from the huge research work needed if each parameter effect is studied individually while the rest are remained constant. This will trigger trillions of experimental or numerical work even if each parameter changes only 3 times. Moreover, it is interesting to be noted that the influences of these parameters may be crossover and coupled. For example, the dimensionless combination of ($nF\eta/RT$) is often used in the design or simulation of PEMFC to determine the electrical current. As long as this combination keeps the same, the electrical current will not change no matter how much variation of the individual parameters of the combination changes. The importance and function of such dimensionless parameters in the study of fuel cell have not been fully revealed and understood. Therefore even though so many papers have been published and great advances in technologies have been received, the importance of different dimensional parameters on the PEMFC performance are remained unresolved and the way of study should be improved to greatly reduce the workload either experimental or numerical. Reformation to the modeling research method of fuel cell is urgently required.

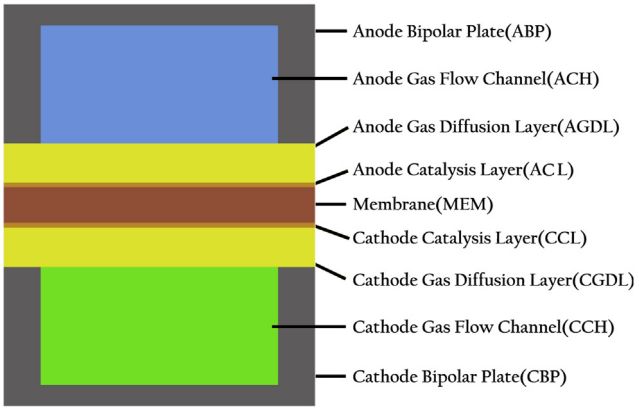

Fig. 1 – Cross section of PEMFC.

Similarity theory is a classical but an effective tool for the research of general laws. When the experimental data are formulated in the form of similarity criteria, individual experimental results will represent the whole similarity group, which will greatly save the experimental workload. Since it was proposed in 1914 [25,26], similarity principle has been applied widely in the research of basic law in the fields of flow and heat transfer [27], mechanics [28], electrochemical [29], and so on. In the past two decades, a number of researchers have been aware of the importance of applying similarity theory in the study of PEMFC [30–42]. Typical examples are as follows. The dimensional analysis method is used to analyze the two-phase transport in a PEMFC by Wang and Chen [31], and the Damkohler number is adopted to characterize the results. Gyenge [38] applies the dimensional analysis method to derive the dimensionless number for the performance study of the membrane electrode, cathode catalyst layer and diffusion layer. It is concluded that a dimensional analysis-based approach coupled with a mathematical model of the fuel cell could be used to quantify and analyze new experimental data for a wide range of conditions. Cho et al. adopted dimensional analysis [39] to extend the

* Nomenclatures of other symbols are shown in Table 2.

research by scaling the relationship between the in situ and ex situ measurements. Three groups of post scaling relationships between Pt coverage and contaminant concentration appear in a single line while the data before scaling are highly scattered. Protsenko and Danilov [40] make a comprehensive analysis for the electrode kinetics by PI theorem and three criteria were obtained. Their results show that similarity theory is applicable for a kinetic analysis of an electrochemical reaction. A non-dimensional analysis of PEM fuel cell phenomena is conducted by means of AC impedance measurement [41] which is used to characterize the electrochemical reaction within PEMFC. Several researches developed dimensionless analysis on approximate solution of cathode catalyst layer (CCL) performance modeling and derived an analytical polarization curve of PEMFC cathode side [43]. Parameters in the analytical polarization curve were fitted based on published polarization data.

All the above studies make their own contribution in the application of the similarity theory to study the performance of different parts of a PEMFC. However, because of the process complexity of PEMFC, there are few studies on the dimensionless polarization curve based on a complete PEMFC model, which is the most important integrated character of PEMFC. Recently, authors of the present paper have tried this approach for a 3D single phase model of a PEMFC [6] and obtained some important results. The purpose of this paper is to present our analysis method, results and discussion. It should be noted that in references both terminologies of similarity theory [26,27,44,45] or dimensional analysis [28,29,41] have been used. In this paper they are regarded as identical in essence and in the following presentation, only the terminology of similarity theory is used for simplicity.

The rest of the paper is organized as follows. In Section Derivation of similarity criterion nine dimensionless numbers, including seven criteria from the input parameters and two dimensionless numbers measuring the output characteristics, are derived by equation analysis method for the 3-dimensional single-phase isothermal model, which is the most basic PEMFC mathematical model. In Section Results and discussion, numerical simulations results are presented and discussed. Discussion is implemented along three aspects. First the comparison between dimensional and dimensionless polarization curve is conducted. Then the feasibility of the proposed dimensionless polarization curve is tested for variety of variation of the input parameters. Third the sensitivities of the obtained criteria of the polarization curve are examined. In Section Conclusion the major contributions and the main observations are concluded.

Derivation of similarity criterion

Similarity analysis for governing equations

3D single-phase isothermal PEMFC mathematical model adopted in Ref. [6] is listed in Table 1. According to [27,44,45] for process with established governing equations, the dimensionless criteria can be derived by equation analysis method for which the details will be implemented latter. For conciseness, all formulas in this paper follow Einstein's summation convention. All parameters and the reference values are listed in Table 2. In the following this equation analysis method is applied to three conservation equations of this model.

Followings are the derivation process of the similarity criteria from the above governing equations.

(1) Momentum equations in a porous medium.

It can be described as follows

$$\frac{1}{\varepsilon^2}\rho u_i\frac{\partial u_j}{\partial x_i}=-\frac{\partial p}{\partial x_j}+\frac{1}{\varepsilon}\mu_e\frac{\partial}{\partial x_i}\left(\frac{\partial u_j}{\partial x_i}\right)-\frac{\mu}{K}u_j \tag{1}$$

where x_i is the direction component, u_i is the superficial velocity in a porous medium which is defined by

$$u_i=u_{i,\text{superficial}}=\varepsilon u_{i,\text{physical}} \tag{2}$$

Consider two PEMFC systems shown by single prime and double prime in superscript of each variables, respectively:

$$\frac{1}{\varepsilon'^2}\rho' u_i'\frac{\partial u_j'}{\partial x_i'}=-\frac{\partial p'}{\partial x_j'}+\frac{1}{\varepsilon'}\mu_e'\frac{\partial}{\partial x_i'}\left(\frac{\partial u_j'}{\partial x_i'}\right)-\frac{\mu'}{K'}u_j' \tag{3}$$

$$\frac{1}{\varepsilon''^2}\rho'' u_i''\frac{\partial u_j''}{\partial x_i''}=-\frac{\partial p''}{\partial x_j''}+\frac{1}{\varepsilon''}\mu_e''\frac{\partial}{\partial x_i''}\left(\frac{\partial u_j''}{\partial x_i''}\right)-\frac{\mu''}{K''}u_j'' \tag{4}$$

Define proportionality coefficients

$$\begin{aligned}&\rho'/\rho''=C_\rho,\ u_i'/u_i''=C_u,\ x_i'/x_i''=C_x,\ p'/p''=C_p\\&\mu'/\mu''=C_\mu,\ \mu_e'/\mu_e''=C_{\mu_e},\ \varepsilon'/\varepsilon''=C_\varepsilon,\ K'/K''=C_K\end{aligned} \tag{5}$$

Substitute Eq. (5) into Eq. (3), yielding

$$\begin{aligned}\frac{1}{\varepsilon''^2}\rho''u_i''\frac{\partial u_j''}{\partial x_i''}=&-\left(\frac{C_\varepsilon^2C_x}{C_\rho C_u^2}\frac{C_p}{C_x}\right)\frac{\partial p''}{\partial x_j''}+\left(\frac{C_\varepsilon C_x}{C_\rho C_u^2}\frac{C_{\mu_e}C_u}{C_x^2}\right)\frac{1}{\varepsilon''}\mu_e''\frac{\partial}{\partial x_i''}\left(\frac{\partial u_j''}{\partial x_i''}\right)\\&-\left(\frac{C_\varepsilon^2C_x}{C_\rho C_u^2}\frac{C_\mu C_u}{C_K}\right)\frac{\mu''}{K''}u_j''\end{aligned} \tag{6}$$

Comparing Eq. (6) with Eq. (4), similarity principle requires

$$\begin{aligned}&\frac{C_\varepsilon C_x}{C_\rho C_u^2}\frac{C_{\mu_e}C_u}{C_x^2}=\frac{C_\varepsilon C_{\mu_e}}{C_\rho C_u C_x}=1,\ \frac{C_\varepsilon^2C_x}{C_\rho C_u^2}\frac{C_p}{C_x}=\frac{C_\varepsilon^2C_p}{C_\rho C_u^2}=1\\&\left(\frac{C_\varepsilon C_x}{C_\rho C_u^2}\frac{C_{\mu_e}C_u}{C_x^2}\right)\Big/\left(\frac{C_\varepsilon^2C_x}{C_\rho C_u^2}\frac{C_\mu C_u}{C_K}\right)=\frac{C_KC_{\mu_e}}{C_\varepsilon C_x^2C_\mu}=1\end{aligned} \tag{7}$$

Then following results are yielded:

$$\left(\frac{\varepsilon\mu_e}{\rho ux}\right)'=\left(\frac{\varepsilon\mu_e}{\rho ux}\right)'',\ \left(\frac{\varepsilon^2\Delta p}{\rho u^2}\right)'=\left(\frac{\varepsilon^2\Delta p}{\rho u^2}\right)'',\ \left(\frac{K\mu_e}{\varepsilon x^2\mu}\right)'=\left(\frac{K\mu_e}{\varepsilon x^2\mu}\right)'' \tag{8}$$

The obtained three dimensionless numbers are termed as,

$$\Pi_1=Re=\frac{\rho ux}{\varepsilon\mu_e},\ \Pi_2=Eu=\frac{\varepsilon^2\Delta p}{\rho u^2},\ \Pi_3=Dar=\frac{K\mu_e}{\varepsilon x^2\mu}=\frac{K\mu_r}{\varepsilon x^2} \tag{9}$$

(2) Species density conversion equations in anode catalyst layer (ACL)

It can be described by

Table 1 – Mathematical formulation of 3D single-phase isothermal PEMFC model.

Governing equations	Source terms
Mass conservation equation $\frac{\partial(\rho u_i)}{\partial x_i} = S_{mass}$	$S_{mass} = \sum_i S_i, i = H_2, O_2, vapor$
Momentum conservation equations $\frac{\rho}{\varepsilon^2}u_i\frac{\partial u_j}{\partial x_i} = -\frac{\partial p}{\partial x_j} + \frac{\mu_e}{\varepsilon}\frac{\partial}{\partial x_i}\left(\frac{\partial u_j}{\partial x_i}\right) + S_{u,j}$	$S_{u,j} = -\frac{\mu}{K}u_j$
Species density conservation equation: $u_i\frac{\partial \rho_j}{\partial x_i} = \frac{\partial}{\partial x_i}\left(D_{ij,eff}\frac{\partial \rho_j}{\partial x_i}\right) + S_j, j = H_2, O_2, vapor$	$S_H = \begin{cases} -(i_a/2F)M_H, ACL \\ 0 \quad , other \end{cases}$ $S_O = \begin{cases} -(i_c/4F)M_O, ACL \\ 0 \quad , other \end{cases}$ $S_{vapor} = \begin{cases} -(\beta i_a/F)M_{H_2O} \quad , ACL \\ [(1+2\beta)i_c/2F]M_{H_2O}, CCL \\ 0 \quad , other \end{cases}$
Electronic potential conservation equation: $\frac{\partial}{\partial x_i}\left(\sigma_s\frac{\partial \phi_s}{\partial x_i}\right) + S_{\phi,s} = 0$	$S_{\varphi,s} = \begin{cases} -i_a, ACL \\ i_c, CCL \\ 0, other \end{cases}$
Ionic potential conservation equation: $\frac{\partial}{\partial x_i}\left(\sigma_m\frac{\partial \phi_m}{\partial x_i}\right) + S_{\phi,m} = 0$	$S_{\varphi,m} = \begin{cases} i_a, ACL \\ -i_c, CCL \\ 0, other \end{cases}$
Boundary conditions	**Calculation relation for electrical current i**
$u_{k,in} = St_k\left(\frac{J_{ref}}{n_k F}\right)\left(\frac{RT_{in}}{p_{k,in}}\right)\left(\frac{1}{\omega_{k,in}}\right)\left(\frac{A_{mem}}{A_{ch}}\right)$ $k = anode, \ cathode$ $\phi_s = \eta_t, anode \ terminal$ $\phi_s = 0, cathode \ terminal$ $\frac{\partial \phi_m}{\partial n} = 0, anode \ and \ cathode \ terminals$	$i_a = A_s J_0^a (c_H^m/c_{H,ref}^m)^{1/2}[\exp(\alpha_a n_a F\eta_a/RT) - \exp(-\alpha_c n_a F\eta_a/RT)]$ $i_c = A_s J_0^c (c_O^m/c_{O,ref}^m)[-\exp(\alpha_a n_c F\eta_c/RT) + \exp(-\alpha_c n_c F\eta_c/RT)]$ $c_i^m = H_i\rho_i/M_i$
Relation for physical properties	
$\mu_e = \mu\mu_r = \mu$ $\rho = \frac{pM}{RT}$	$D = D_0\varepsilon^{1.5}\left(\frac{T}{T_0}\right)^{1.5}\left(\frac{p}{p_0}\right)^{-1}$
Relation for output voltage	
$V_{oc} = 0.0025T + 0.2329$[46]	$V_{cell} = V_{oc} - \eta_t$

$$u_i\frac{\partial \rho_j}{\partial x_i} = D_{ij,eff}\frac{\partial}{\partial x_i}\left(\frac{\partial \rho_j}{\partial x_i}\right) - k_{s,j}\frac{A_s J_{0,a} M_j}{n_j F}\left(\frac{H_H\rho_j}{M_j c_{a,ref}^m}\right)^{1/2}\left[\exp\left(\frac{\alpha_a n_a F\eta_a}{RT}\right) - \exp\left(-\frac{\alpha_c n_a F\eta_a}{RT}\right)\right], j = H_2, vapor; k_{s,H} = 1, k_{s,vapor} = \beta \quad (10)$$

It should be noted that even if the applied model is termed as single phase model the water of its gas state in the catalyst layer and liquid state in the membrane is still treated differently. Here actually single phase means that in the gas diffusion layer and in the bi-polar plate channel water is treated as single phase (vapor).

As indicated above the exponential term itself is a dimensionless parameter,

$$\Pi_4 = \frac{RT}{\alpha n F\eta} \quad (11)$$

For the derivation of similarity criteria, two PEMFC systems can be described by

Table 2 – Model parameters and their reference values.

No.	Symbol	Parameter	Value or/and unit
1	$A_sJ_{0,a}$	Exchange current density times specific area in anode	$2.0 \times 10^8 A \cdot m^{-3}$
2	$A_sJ_{0,c}$	Exchange current density times specific area in cathode	$1.6 \times 10^2 A \cdot m^{-3}$
3	$c^m_{a,ref}$	H_2 reference concentration in the Nafion	$56.4\ mol \cdot m^{-3}$
4	$c^m_{c,ref}$	O_2 reference concentration in the Nafion	$3.39\ mol \cdot m^{-3}$
5	$D_{H,ref}$	Reference diffusivity of H_2 in gas (1 atm, 307 K)	$0.915\ cm^2 \cdot s^{-1}$
6	$D_{O,ref}$	Reference diffusivity of O_2 in gas (1 atm, 293 K)	$0.220\ cm^2 \cdot s^{-1}$
7	$D_{vapor,ref}$	Reference diffusivity of vapor in gas (1 atm, 307 K)	$0.256\ cm^2 \cdot s^{-1}$
8	F	Faraday constant	$96485C \cdot mol^{-1}$
9	h_{ch}	Gas channel height	$7.62\times10^{-4}m$
10	h_d	Diffuser layer thickness	$2.5410^{-4}m$
11	h_{cat}	Catalyst layer thickness	$2.87 \times 10^{-5}m$
12	h_{mem}	Membrane thickness	$2.3 \times 10^{-4}m$
13	H_H	Henry constant of H_2 in the Nafion	0.64
14	H_O	Henry constant of O_2 in the Nafion	0.19
15	J_{cell}	Output current density	$A \cdot m^{-2}$
16	K_{gdl}	Permeability of gas diffusion layer	$1.76 \times 10^{-11}m^2$
17	K_{cl}	Permeability of catalyst layer	$1 \times 10^{-14}m^2$
18	L_c	Gas channel length	0.07112 m
19	L_t	Distance between anode and cathode terminals	0.0025914 m
20	M	Molar mass	$kg \cdot mol^{-1}$
21/22/23	n	Electron number of electrochemical reaction	$H_2/O_2/H_2O$
24/25	p_a/p_c	Anode/cathode pressure (absolute pressure)	3/5atm
26	R	Gas constant	$8.314J \cdot mol^{-1} \cdot K^{-1}$
27/28	RH_a/RH_c	Relative humidity of inlet fuel/air	100%/0%
29/30	St_a/St_c	Fuel/air stoichiometric flow ratio	3/3
31	T	Temperature	353K
32	u_i	Superficial velocity	$m \cdot s^{-1}$
33	V_{cell}	Output voltage	V
34	V_{oc}	Open circuit voltage	V
35	W	Gas channel width	0.001524 m
36	W_{BP}	Bipolar plate width	0.002 m
37	α_a	Anode transfer coefficient	1
38	α_c	Cathode transfer coefficient	0.5
39	β	Net water transfer rate	0.2
40	ε_{gdl}	Gas diffusion layer porosity	0.4
41	ε_{cat}	Catalyst layer porosity	0.28
42	η_t	Overpotential in anode terminal	V
43	μ_e	Effective viscosity in a porous medium	Pa·s
44	ρ	Density	$kg \cdot m^{-3}$
45	σ_s	Solid phase conductivity	$90S \cdot m^{-1}$
46	σ_m	Membrane phase conductivity	$17S \cdot m^{-1}$
47	ω_0	Oxygen mass fraction of inlet air	0.233

$$u_i'\frac{\partial\rho_j'}{\partial x_i'} = D'_{ij,eff}\frac{\partial}{\partial x_i'}\left(\frac{\partial\rho_j'}{\partial x_i'}\right) - k'_{s,j}\frac{H_H^{1/2}M_j^{1/2}}{n_jF}\rho_j'^{1/2}\left(\frac{A_sJ_{0,a}}{c^{m\ 1/2}_{a,ref}}\right)' \quad (12)$$

$$u_i''\frac{\partial\rho_j''}{\partial x_i''} = D''_{ij,eff}\frac{\partial}{\partial x_i''}\left(\frac{\partial\rho_j''}{\partial x_i''}\right) - k''_{s,j}\frac{H_H^{1/2}M_j^{1/2}}{n_jF}\rho_j''^{1/2}\left(\frac{A_sJ_{0,a}}{c^{m\ 1/2}_{a,ref}}\right)'' \quad (13)$$

Take the same derivation process as for Eq. (1), we have following equations in succession

$$\rho_i'/\rho_i'' = C_\rho,\ u_i'/u_i'' = C_u,\ x_i'/x_i'' = C_x,\ k'_{s,i}/k''_{s,i} = C_k,\ D'/D'' = C_D,$$

$$\left(\frac{A_sJ_{0,a}}{c^{m\ 1/2}_{a,ref}}\right)'\Big/\left(\frac{A_sJ_{0,a}}{c^{m\ 1/2}_{a,ref}}\right)'' = C_A \quad (14)$$

$$\left(\frac{C_uC_\rho}{C_x}\right)\left(\frac{C_x^2}{C_DC_\rho}\right)u_i''\frac{\partial\rho_j''}{\partial x_i''} = (D_{ij,eff})'\frac{\partial}{\partial x_i''}\left(\frac{\partial\rho_j''}{\partial x_i''}\right) - \left(\frac{C_x^2}{C_DC_\rho}\right)C_kC_AC_\rho^{1/2}k''_{s,j}\frac{H_H^{1/2}M_j^{1/2}}{n_jF}\rho_j''^{1/2}\left(\frac{A_sJ_{0,a}}{c^{m\ 1/2}_{a,ref}}\right)'' \quad (15)$$

$$\left(\frac{C_x^2}{C_DC_\rho}\right)C_kC_A(C_\rho)^{1/2} = \frac{C_kC_x^2C_A}{C_DC_\rho^{1/2}} = 1,\ \left(\frac{C_uC_\rho}{C_x}\right)\left(\frac{C_x^2}{C_DC_\rho}\right) = \frac{C_xC_u}{C_D} = 1 \quad (16)$$

$$\left(\frac{k_{s,i}A_sJ_{0,a}x^2}{c^{m\ 1/2}_{a,ref}D\rho_H^{1/2}}\right)' = \left(\frac{k_{s,i}A_sJ_{0,a}x^2}{c^{m\ 1/2}_{a,ref}D\rho_H^{1/2}}\right)'',\ \left(\frac{D}{xu}\right)' = \left(\frac{D}{xu}\right)'' \quad (17)$$

Two dimensionless numbers are obtained

$$\Pi_5 = Dam = \frac{H_H^{1/2} M_j^{1/2}}{n_j F} \frac{k_{s,j} A_s J_{0,a} x^2}{c_{a,ref}^{m\ 1/2} D \rho_H^{1/2}},\ j = H_2, \text{vapor}; k_{s,H} = 1, k_{s,\text{vapor}} = \beta,\ \Pi_6 = \frac{D}{xu} \tag{18}$$

Similar derivation for $j = O_2$ of Eq. (10) gives Damkohler number in CCL

$$\Pi_5 = Dam = \frac{H_O}{n_j F} \frac{k_{s,j} A_s J_{0,c} x^2}{c_{c,ref}^m D},\ \ j = O_2, \text{vapor},\ \ k_{s,O} = 1, k_{s,\text{vapor}} = 1 + 2\beta \tag{19}$$

(3) Potential conversation equations in anode catalyst layer

It can be described by

$$\sigma_j \frac{\partial}{\partial x_i}\left(\frac{\partial \phi_j}{\partial x_i}\right) - k_{\sigma,j} A_s J_0^a \left(\frac{H_H \rho_H}{M_H c_{H,ref}^m}\right)^{1/2} \left[\exp\left(\frac{\alpha_a n_a F \eta_a}{RT}\right) - \exp\left(-\frac{\alpha_c n_a F \eta_a}{RT}\right)\right] = 0$$

$$j = s, m; k_{\sigma,s} = 1, k_{\sigma,m} = -1 \tag{20}$$

Take the same process, finally we yield conduction number in anode and cathode.

$$\Pi_{7,\text{Anode}} = \left(\frac{H_H}{M_H}\right)^{1/2} \left(\frac{A_s J_{0,a} \rho_H^{1/2} x^2}{c_{H,ref}^{m\ 1/2} \sigma_i \phi_i}\right) \tag{21}$$

$$\Pi_{7,\text{Cathode}} = \frac{H_O A_s J_{0,c} \rho_O x^2}{M_O c_{O,ref}^m \sigma_i \phi_i} \tag{22}$$

Seven kinds of dimensionless criterions, shown in Eq. (9), (11), (18), (19), (21) and (22), related to the input parameters are derived. It can be shown that from the governing equations listed in Table 1 only the above seven kinds of similarity criterions can be derived.

Come here to discuss the physical significances of these dimensionless numbers. Π_1 is the well-known Reynolds number which is a measure of the relative importance between inertial effect and viscous effect. Π_2 is the Euler number which is a measure of the relative magnitude between static pressure drop and dynamic pressure. These two dimensionless numbers mainly play roles in the gas flow channels. Π_3 is the Darcy number representing a ratio of flow resistance due to a porous medium and the diffusion term effect. Π_4 is a measure of the effect of temperature and activity overpotential on the electrochemical reaction rate. Π_5 is the Damkohler number which represents a ratio between reference reaction rate and diffusion mass transfer. These two numbers react in catalytic layers. Π_6 is a measure of the relative importance of diffusion mass transfer over convection mass transfer, which takes effect in gas diffusion layers and catalyst layers. Π_7 is a relative magnitude of reference reaction rate versus conductivity rate, which reacts on all potential layers. $\Pi_{1\text{-}3}$ are criteria about the flow field. Π_4, $\Pi_{5,6}$, Π_7 represent the most important three loss in PEMFC, polarization potential loss, mass transport loss and Ohmic loss respectively.

Definitions of dimensionless voltage and current

As indicated above one major purpose of the present study is to construct a non-dimensional polarization curve. To proceed, the two output parameters, voltage and electrical current, should be nondimensionalized. They are defined as follows.

The dimensionless voltage is defined as a ratio of the magnitude of the output voltage over the overpotential,

$$\Pi_8 = \bar{V}_{cell} = \frac{V_{cell}}{\eta_t} = \frac{V_{oc}}{\eta_t} - 1 \tag{23}$$

To define the dimensionless current density a referenced value should be found. It can be derived from the boundary condition of the electric potential as follows.

Output current density can be calculated for cathode by Ohm's law

$$J = -\sigma \frac{\partial \phi}{\partial l} = \int i dl = \int \frac{H_O}{M_O} \frac{\rho_O A_s J_{0,c}}{c_{c,ref}^m} \left[-\exp\left(\frac{\alpha_a n_c F \eta_c}{RT}\right) + \exp\left(-\frac{\alpha_c n_c F \eta_c}{RT}\right)\right] dl \tag{24}$$

where l is the through-plane direction of the membrane.

Considering two systems

$$J' = \int \frac{H_O'}{M_O} \frac{\rho_O' A_s' J_{0,c}'}{c_{c,ref}^{m\ \prime}} dl' \tag{25}$$

$$J'' = \int \frac{H_O''}{M_O} \frac{\rho_O'' A_s'' J_{0,c}''}{c_{c,ref}^{m\ \prime\prime}} dl'' \tag{26}$$

Assuming proportionality coefficients

$$C_J = J'/J'', C_\rho = \rho'/\rho'', C_A = (A_s J_{0,c})'/(A_s J_{0,c})'', C_c = c_{c,ref}^{m\ \prime}/c_{c,ref}^{m\ \prime\prime}, C_l = l'/l''$$

$$C_H = H_O'/H_O'',\ \ C_M = M_O'/M_O'' \tag{27}$$

Substituting Eq. (27) into Eq. (25)

$$J'' = \frac{C_\rho C_A C_l C_H}{C_c C_J C_M} \int \frac{H_O''}{M_O''} \frac{\rho_O'' A_s'' J_{0,c}''}{c_{c,ref}^{m\ \prime\prime}} dl'' \tag{28}$$

Comparing Eq. (28) and Eq. (26)

$$\frac{C_\rho C_A C_l C_H}{C_c C_J C_M} = 1 \tag{29}$$

$$\left(\frac{M_O J c_{c,ref}^m}{H_O A_s J_{0,c} \rho_O x}\right)' = \left(\frac{M_O J c_{c,ref}^m}{H_O A_s J_{0,c} \rho_O x}\right)'' \tag{30}$$

We obtain the dimensionless number of output characteristic

$$\Pi_9 = \bar{J}_{cell} = \frac{J_{cell} M_O c_{O,ref}^m}{H_O A_s J_0 \rho_{O,in,c} L_t} = \frac{J_{cell}}{H_O A_s J_0 \rho_{O,in,c} L_t / M_O c_{c,ref}^m} \tag{31}$$

Thus the referenced electrical current density can be defined as

$$J_{cell,0} = \frac{H_O A_s J_0 \rho_{O,in,c} L_t}{M_O c^m_{c,ref}} \quad (32)$$

The dimensionless cell current density can be re-written by

$$\bar{J}_{cell} = \frac{J_{cell}}{J_{cell,0}} \quad (33)$$

Determining parameter values in criteria

In order to apply the above analysis results, all parameters included in the dimensionless criteria should be claimed by the way of their determination. The parameters involved in the derived criteria can be divided into four categories, and the way of their determination are recommended as follows.

(1) Geometrical. The characteristic length of *Re* number is defined by equivalent diameter of gas flow channel, while the length in other five (Π_3, Π_5, Π_6, Π_7, Π_9) takes the distance between anode and cathode terminal, denoted by L_t. Porosities in Π_1 and Π_2 take 1 in general. The porosity and permeability in Π_3 takes the given value.
(2) Physical. All the physical properties, μ, μ_e, D, $\sigma_{s,m}$, $H_{H/O}$, are determined by the operational pressure and temperature.
(3) Electrochemical. The electrochemical parameters, α, n, β, $A_s J_0, c^m_{ref}$, take the given data.
(4) Operational. The values of these parameters are suggested as follows: $u_i = u_{i,in}$, $T = T_0$. ρ in Π_1 and Π_2 take the gas density in the flow channel inlet while ρ in Π_7 and Π_9 is defined by the corresponding component density in the inlet. Δp is defined by pressure drop of the gas flow channel.

Results and discussion

In this section numerical results of the dimensionless polarization curve and a number of variations are provided to show the feasibility and reliability of the similarity theory in the study of PEMFC performance.

Dimensionless polarization curve

First the polarization curves of dimensional and dimensionless form for the same PEMFC are compared. Based on the referenced values listed in Table 2 for the single-phase model numerical results of dimensional and dimensionless ones can be created and are shown in Figs. 2(a) and (b), respectively. It can be seen that the range of dimensionless voltage ranges from 0 to infinity, in contrast with the dimensional one from 0 to V_{oc}. This is resulted from the fact that the minimum value of η_t is zero. In addition, the open-circuit voltage in Curve (a) corresponding to an infinity point: $\bar{J} = 0$, $\overline{V} = +\infty$. It is interesting to note that one dimensional polarization curve can only represent the output character of one group of specific values of the involved parameters, while one point in dimensionless polarization curve represents the output character of many individual situations who have the same values of the involved similarity criteria. For example, Curve (a) in Fig. 2 is the simulation results for the specific situation with values of parameter shown in Table 2, while the point of $\overline{V} = 0.812$ in Curve (b) can represent for all situations whose seven criteria are

$$\Pi_{1,A/C} = 9.2/75.5,\ \Pi_{2,A/C} = 180.9/32.1,\ \Pi_3 = 6.55 \times 10^{-6},\ \Pi_4 = 0.0247,$$
$$\Pi_{5,A/C} = 0.533/7.10 \times 10^{-6},\ \Pi_{6,A/C} = 0.165/0.0328,$$
$$\Pi_{7s,A/C} = 39.23/3.90 \times 10^{-5},\ \Pi_{7m,A/C} = 207.70/2.063 \times 10^{-4}$$

where $\Pi_{1,A/C} = 9.2/75.5$ means the Π_1 criterion has its values in anode and cathode of 9.2 and 75.5, respectively. This

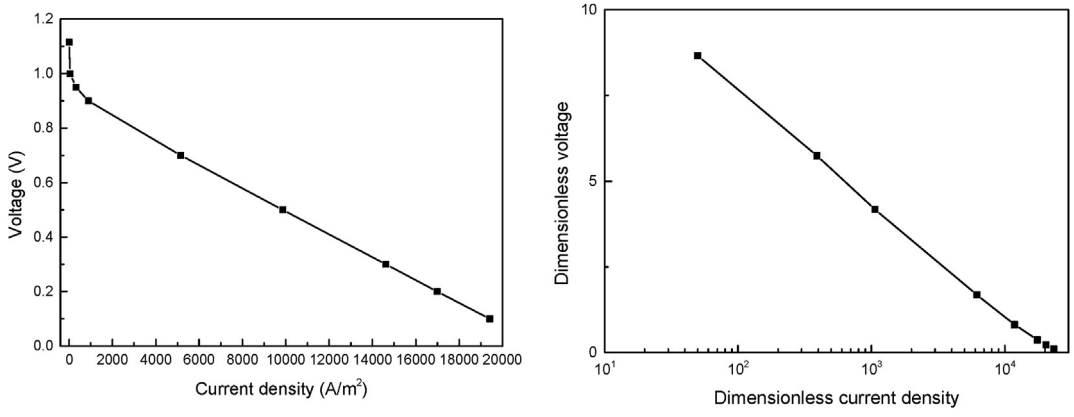

Fig. 2 – Comparison of the polarization curves.

example shows such an important concept: the result of individual test or simulation once expressed in the form of similarity criteria the dimensionless result then ascends to the level of representing the whole similar group. This important feature should be very useful to greatly save both numerical and experimental work for the study and design of fuel cell.

It should be noted here that the mutual transformation between the dimensionless polarization curve and the dimensional one is easy to be implemented in the voltage-given simulation due to the fact that all the parameters in the definitions of dimensionless voltage and electrical current, Eqs. (23) and (32), are pre-determined.

Validation of the numerical model

The basic numerical model in this paper is verified by comparing with Ticianelli's experimental polarization curve [2], and the agglomerate model in cathode catalyst layer adopted in Ref. [6] is used which can be expressed as follows

$$i' = \theta i \tag{34}$$

$$\theta = \frac{\tanh M_T}{M_T} \tag{35}$$

$$M_T = L_{ct}\sqrt{k \Big/ D_{O_2}^m} \tag{36}$$

$$k = \frac{i}{nFc_i^m} \tag{37}$$

where M_T is Thiele modulus, L_{ct} is the characteristic length of catalyst particle (1 μm), $D_{O_2}^m$ is the diffusion coefficient of oxygen in the Nafion polymer (1.22×10^{-10} m^2/s) and k is the reaction rate constant. As shown in Fig. 3, the simulated polarization curve shows its good agreement with experiment data. The maximum relatively deviation is 4.2% when current density is lower than 8000 A/m^2, showing the reliability of the basic numerical model in the single-phase operating region.

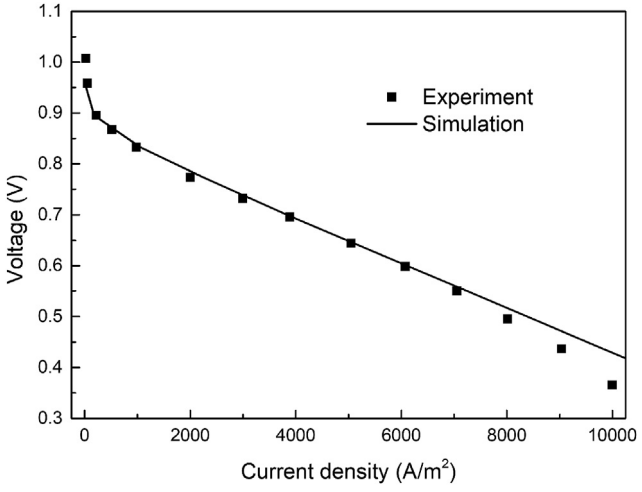

Fig. 3 – Comparison of numerical model prediction polarization curve with experimental data in Ref. [2].

Further numerical validation of the feasibility of dimensionless polarization curve

To the authors' knowledge, in the similarity theory there are three ways to verify whether the derived criteria are correct and reliable. One way is to use the derived criteria for data reduction. If the test or numerical data are very scattered in dimensional expression while they can be represented by one smooth curve by reduction with dimensionless criteria, then the usefulness and correctness of the derived criteria are validated. For example, the serpentine flow field is widely used in PEMFC. When reactant gases flow along the serpentine flow field, there is a pressure drop between the adjacent channels, which produces an under–rib flow of fluid from higher pressure side to the lower pressure side through the GDL. The authors of Ref. [30] measured this under-rib flow rate at different channel inlet flow rates, and expressed in a picture with dimensional underflow rate versus pressure drop as the ordinate and abscissa respectively. A very scattered picture of the data was obtained. Then they used two dimensionless parameters obtained by dimensionless analysis to reduce the data, the test data from different channel flow inlet rates show very consistent variation trend (Figs. 4 and 5 of [30]), showing that their derived criteria are reliable and applicable. The second way is to show the identity of the results when experimental test or numerical simulation are performed by keeping the related criteria constant but changing their components in a quite wide range. If the test or numerical results are reduced by the derived criteria and an identical curve can be obtained, then the feasibility and validity of the obtained criteria are testified. The third way is to show the identity of dimensionless variable distributions for different cases with the same criteria. The second and third ways are now used to verify the correctness of our results.

In the current stage, it is very difficult to validate the result by the experimental approach. This is because that in general, in PEMFC experiment, it is quite possible to change the operator parameters (such as temperature, pressure, humidity and stoichiometric ratio) and geometric parameters. However, because the seven derived criteria are complex, containing physical property parameters and electrochemistry parameters, which are hardly changeable freely in the experiment. Therefore, it is very difficult to design one group of experiment to guarantee all the major criteria keep the same. Tremendous work is needed to get the correspondent experimental results. Numerical method in conjunction with experimental validation is an effective approach in PEMFC study, which has been proposed and developed by many researchers for more than ten years so far. Numerical simulations for two scenarios (Scenario 1, Scenario 2) and the dimensionless current distribution of Scenario 2 are conducted and their results are presented below.

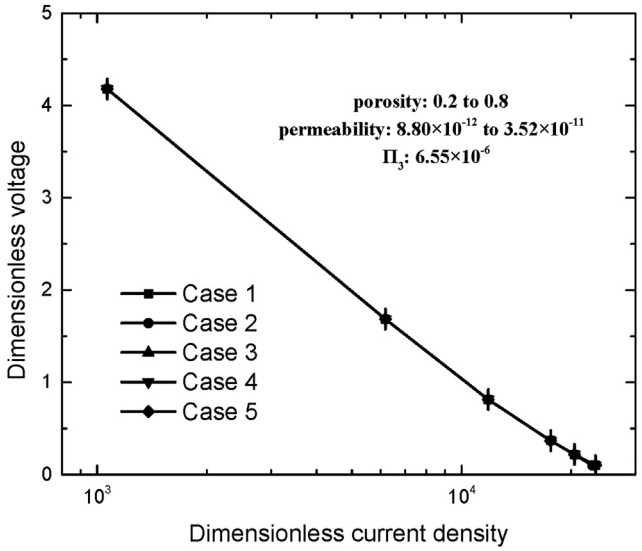

Fig. 4 – Numerical verification result for similarity criteria Π_3 (Scenario 1) (For data details see Table S1).

3-3-1. *dimensionless polarization curve of the first scenario*
In the first scenario, porosity and permeability in gas diffusion layers are changed under the premise of the identity of *Dar* (Π_3). The parameter variation details are given in Table S1. In the table the first two lines present the changed parameters, and each parameter changes five times. The rest in the table is the values of the other criteria adopted in this simulation. As can be seen from Table S1, for the five cases studied, the porosity changes within 0.2–0.8, the permeability changes within 8.8×10^{-12} to 3.52×10^{-11}, the values of Π_3 for the five cases remain identical within three digits (6.55×10^{-6}). The five simulated dimensionless polarization curves are shown in Fig. 4, and they agree with each very well (actually overlap with each other). The relative deviation between the five curves is only −0.010% to +0.011%.

3-3-2. *Dimensionless polarization curve of the second scenario*
In the second scenarios, three cases are studied. In the three cases eight component parameters are changed within quite large ranges, and they are changed in such a way that the identity of Π_5, Π_6 and Π_7 are satisfied within three digits. The details of parameter and criteria values are presented in Table S2. The first eight lines show the components variation range, and each varies three times. The predicted dimensionless polarization curves for the three cases also agree with each other very well (see Fig. 5 (a)), with a relative deviation of −1.2% to +1.1% in the vast majority of cases which can be accepted for engineering calculation. In Fig. 5 (b) the corresponding dimensional polarization curves of the three cases are presented and they differs from each other very significantly, demonstrating our previous statement that one dimensionless polarization curve can represent the output character of many individual situations who have the same values of the involved similarity criteria.

3-3-3 *dimensionless current distribution of the second scenario*
Come here to see the predicted current density distributions of the Scenario 2. The dimensional current density distribution contours and vector diagrams of Cases 1–3 are shown in Figs. 6(a),(b),(c) respectively. It can be seen that they are different. After normalized by referenced electrical current density in Eq. (32), dimensionless current density distribution contours and vector diagrams of the three cases become identical and are presented in Fig. 7, which is a typical characteristic of similar phenomena.

Sensitivity analysis of the input criteria on dimensionless polarization curve

In Scenario 2, *Re* (Π_1) and *Eu* (Π_2) are changed in a quite large range while the dimensionless polarization curves are almost coincide each other, indicating that *Re* and *Eu* numbers manifest minor effect on dimensionless polarization curve for the cases studied. Thus sensitivity study of the other criterion

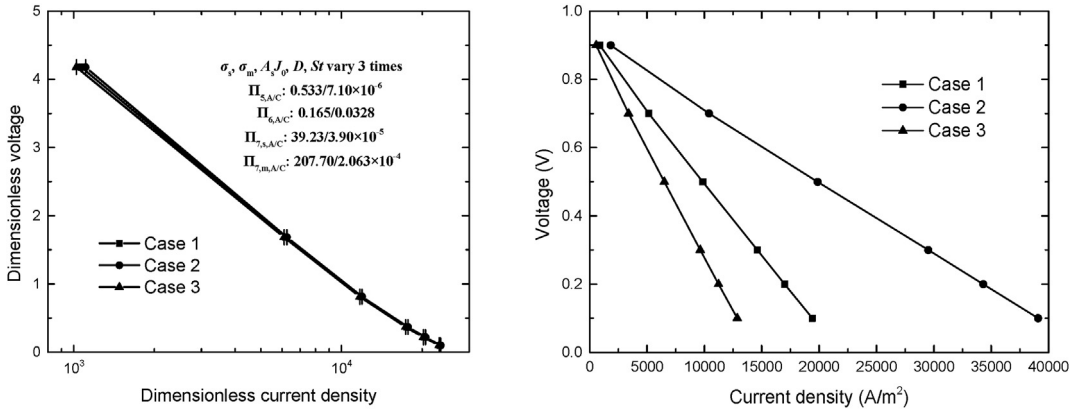

(a) Dimensionless polarization curves (b) Dimensional polarization curves

Fig. 5 – Numerical verification result for similarity criteria $\Pi_{5\sim7}$ (Scenario 2) (For data details see Table S2).

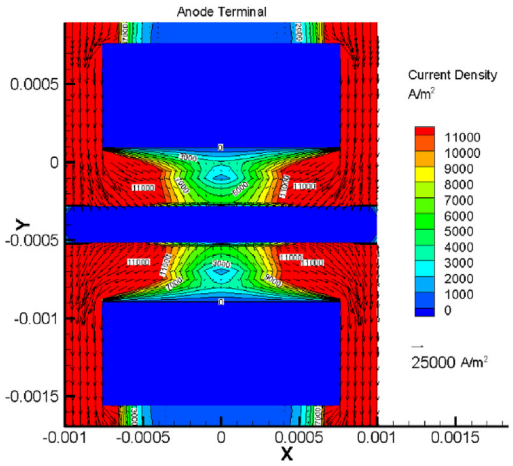

(a) Current density distribution contour and vector diagram of Case 1 at output voltage = 0.5V in the central cross section of the fuel cell

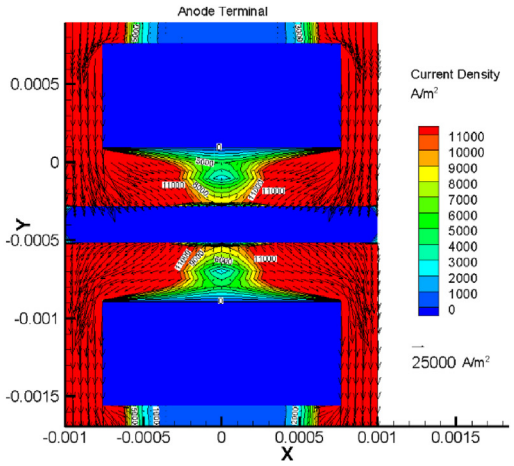

(b) Current density distribution contour and vector diagram of Case 2 at output voltage = 0.5V in the central cross section of the fuel cell

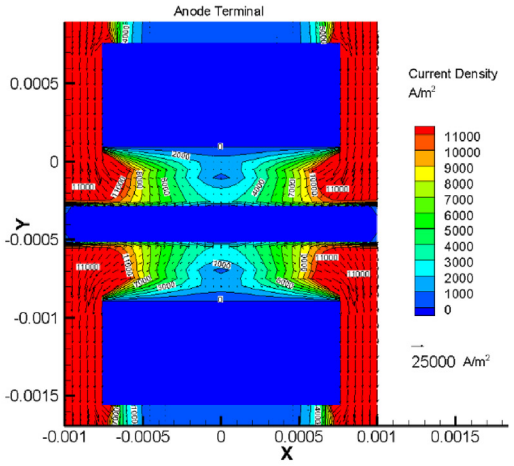

(c) Current density distribution contour and vector diagram of Case 3 at output voltage = 0.5V in the central cross section of the fuel cell

Fig. 6 – Dimensional current distribution of three cases (Scenario 2) (For data details see Table S2).

is needed in order to reveal the important ones and to reduce number of criteria involved for practical application. In the following presentation, the sensitivity of other five dimensionless criteria Π_3~ Π_7 are investigated. Seven groups (Groups 1~7) of numerical simulations are implemented. In each group, some related parameters in Table 2 are changed to guarantee only one dimensionless number changes except *Re* and *Eu*. The parameter variation details of the seven groups are given in Tables S3~S9 respectively. The simulation results are shown in Figs. 8 (a)~(g) respectively.

From Figs. 8 (a)~(g), following features may be noted. First, it can be seen that only Π_4 shows effect on the slope of the dimensionless polarization curve while other criteria show effect on the intercept of the curve with the abscissa. This is due to the fact that only Π_4 appears in the exponential form of the electric current source of the governing equations while other criteria appear in linear form. Second, the effects of the seven kinds of criteria can be divided into three types: great, small and neglected. Π_4 and $\Pi_{7,s}$ show their great influences on the dimensionless polarization curve (−94.9% ~ +349.2%), Π_5 and Π_6 have mild to small effects (−4.5% ~ +5.0%) and the effects of Π_1, Π_2, Π_3 can be totally neglected (−1.2% ~ +1.1%). This is because that Π_4 and Π_7 appear in the most important terms (electrical current source and electrical conductivity)

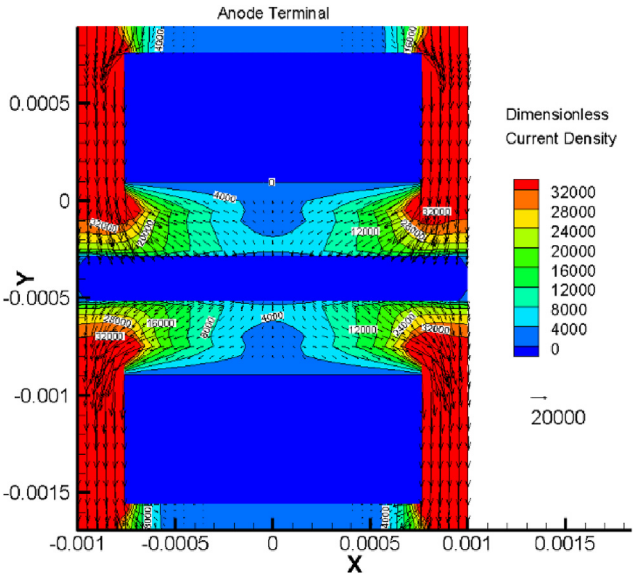

Fig. 7 – Dimensionless current density distribution contours and vector diagrams of Cases 1–3 at output voltage = 0.5V in the central cross section of the fuel cell.

which affects the generation of the electric current. Π_1, Π_2, Π_3 are the similarity criteria about the flow field. For the cases studied, flow characteristics do not have appreciable effect on the fuel cell performance. Π_5, Π_6 affect the mass transfer characteristics in the catalyst layer.

Some special discussion

Finally following important points of this paper are noted and discussed.

(1) The major purpose of this paper is to show the feasibility and applicability of the similarity theory to complicated problem such as fuel cell output characteristics. The adoption of the single-phase isothermal model of PEMFC is because the governing equations of this model are all partial differential equations, from which the equation analysis method can be conveniently used and complete similarity criteria can be obtained. For two-phase situation of PEMFC, even though some sophisticated models have been developed [14,47], they still contain some emperical equation (such as the correlation between capillary pressure and liquid water saturation, Leverett-J function). Therefore to establish a full mathematical model composed by all partial differential equations for PEMFC is an urgent need in the academic study of PEMFC.

(2) The single-phase isothermal model does have its application in engineering, for example, for small power output situation represented by PEMFC unmanned aerial vehicle, and this also why in the early period of PEMFC study, many models were single-phase type, such as [6,46].

(3) As indicated by Churchill early in 1992 [48], the uncertainty associated with similarity analysis arises wholly form the mathematical model on which it based. Therefore the derived similarity criteria should be applicable to the situations when single-phase model is valid.

(4) Different model parameters and empirical formulas can be easy to compare in a wide range [33] based on similarity analysis method, which will benefit to the selection of the model parameters and formulas and promote the development of the PEMFC model.

(5) The similarity theory can also be applied in the simplified PEMFC model, such as one-dimensional model and lumped model. If the governing equations are in the form of differential equation, similarity analysis method (or equation analysis, applied in this paper) is suggested to derive the similarity criteria while if the governing equations are not clear, dimensional analysis method [28] can be adopted. The two methods are regarded as identical in essence [48] and the similarity analysis method is preferentially recommended because similarity analysis method can eliminate the uncertainty associated with the selection of the variables.

Conclusion

The major contributions and observations of this paper can be summarized as follows.

(1) The equation analysis method is adopted to derive the dimensionless criteria for a 3D single-phase model of the complete proton exchange membrane fuel cell model for the first time in the literature, and seven criteria composed of input parameters are obtained.

(2) Dimensionless voltage and dimensionless current density are derived for a complete single fuel cell as output similarity criteria and numerical simulation results of the model are expressed by the dimensionless polarization curve, seemingly first in the literature. Numerical simulation results reveal that as long as the value of each similarity criterion keeps identical, the dimensionless polarization curve remains the same (about 1%) even if the components of the criteria vary 3 times. Furthermore, the mutual transformation between the dimensionless polarization curve and the dimensional one can be easily implemented in the voltage-given simulation due to all the parameters in the above definition are pre-determined. The benefit of similarity theory is illustrated by combining great number of variables into several criteria. Once the results of a numerical or experimental study are presented in dimensionless criteria, they can represent a great number of cases where the related criteria have the correspondent identical values, which will be very useful for greatly saving both numerical and experimental work in the study and design of fuel cell.

(3) For the studied 3D single-phase model of the proton exchange membrane fuel cell, similarity criteria related

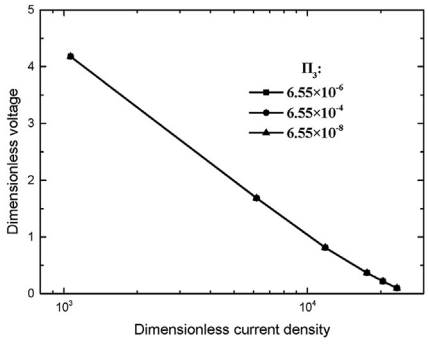

(a) Π_3 (Group 1, for data details see Table S3)

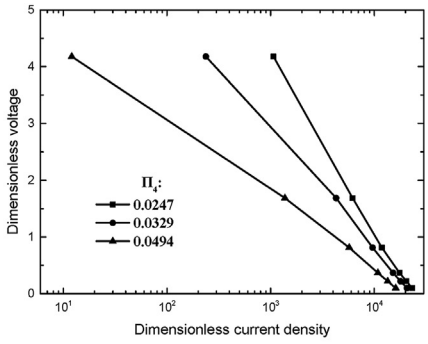

(b) Π_4 (Group 2, for data details see Table S4)

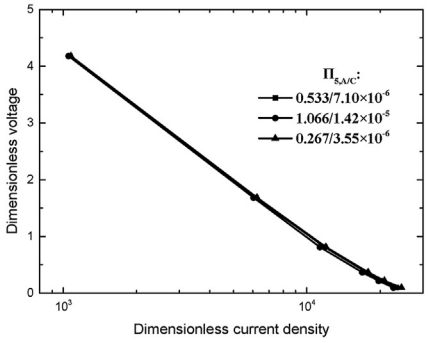

(c) Π_5 (Group 3, for data details see Table S5)

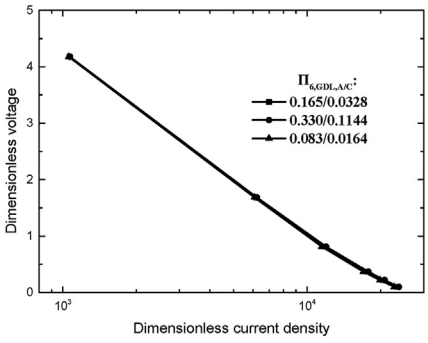

(d) $\Pi_{6,GDL}$ (Group 4, for data details see Table S6)

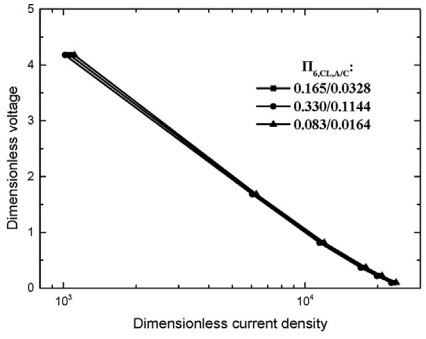

(e) $\Pi_{6,CL}$ (Group 5, for data details see Table S7)

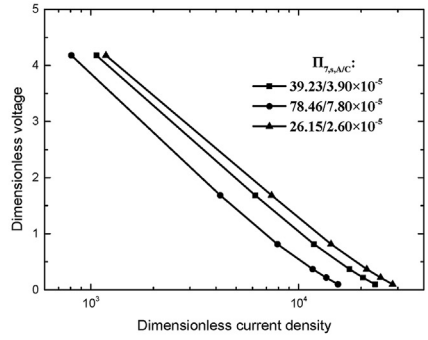

(f) $\Pi_{7,s}$ (Group 6, for data details see Table S8)

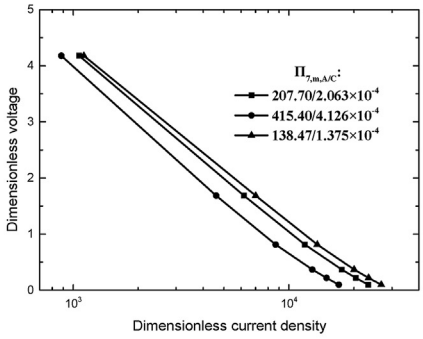

(g) $\Pi_{7,m}$ (Group 7, for data details see Table S9)

Fig. 8 – Sensibility analysis for Π_3~Π_7.

to flow field (Π_1, Π_2, Π_3) shows negligible effects (−1.2% ~ +1.1%) on the dimensionless polarization curve.

(4) For the model studied, dimensionless criteria relative to electrochemical characteristics (Π_4 and Π_7) show strong effects (−94.9% ~ +349.2%) on the dimensionless polarization curve. Criteria with regard to mass transfer characteristics (Π_5 and Π_6) have mild to minor influence (−4.5% ~ +5.0%). Π_4 has high influence on the slope of dimensionless polarization curve while other similarity criteria show effect on the intercept with the abscissa.

Author contributions

Wen-Quan Tao: Conceptualization, Methodology, Resources, Writing - Review & Editing, Supervision, Project administration, Funding acquisition **Fan Bai**: Methodology, Software, Validation, Formal analysis, Investigation, Data Curation, Writing - Original Draft, Visualization **Le Lei**: Investigation **Zhuo Zhang**: Investigation **Hailong Li**: Writing - Review & Editing **Jinyue Yan**: Writing - Review & Editing, Funding acquisition **Li Chen**: Investigation **Yan-Jun Dai**: Investigation **Lei Chen**: Investigation.

Declaration of competing interest

The authors declare that they have no known competing financial interests or personal relationships that could have appeared to influence the work reported in this paper.

Acknowledgment

Funding: Wen-Quan Tao thanks the grants from the Key Project of National Natural Science Foundation of China [Grant number 51836005], the International Exchange Cooperation Project of NSFC-STINT [Grant number 51911530157], the National Key Research and Development Program [Grant number 2017YFB0102702], the Basic Research Project of Shaanxi Province [Grant number 2019ZDXM3-01], the Foundation for Innovative Research Groups of the National Natural Science Foundation of China [Grant number 51721004] and the Key Science and Technology Project in Henan Province (Innovation Leading Project) [Grant number: 191110210200]. Jinyue Yan and Hailong Li acknowledge the support of Program Energy management of fuel cell powered data centers, Sweden [Grant number CH2018-7844]. Funding sources had no involvement in the research and preparation of the article.

Appendix A. Supplementary data

Supplementary data to this article can be found online at https://doi.org/10.1016/j.ijhydene.2021.08.205.

REFERENCES

[1] Bai F., Lei L., Zhang Z., Chen L., Chen L., Tao W.Q. Application of similarity theory in the study of proton exchange membrane fuel cells: A comprehensive review of recent developments and future research requirements. Accepted by Energy Storage and Saving.

[2] Ticianelli EA, Derouin CR, Srinivasan S. Localization of platinum in low catalyst loading electrodes to to attain high power densities in SPE fuel cells. J Electroanal Chem Interfacial Electrochem 1988;251(2):275–95. https://doi.org/10.1016/0022-0728(88)85190-8.

[3] Ticianelli EA, Derouin CR, Redondo A, Srinivasan S. Methods to advance technology of proton exchange membrane fuel cells. J Electrochem Soc 1988;135(9):2209–14. https://doi.org/10.1149/1.2096240.

[4] Yousfi-Steiner N, Moçotéguy P, Candusso D, Hissel D. A review on polymer electrolyte membrane fuel cell catalyst degradation and starvation issues: causes, consequences and diagnostic for mitigation. J Power Sources 2009;194(1):130–45. https://doi.org/10.1016/j.jpowsour.2009.03.060.

[5] Jiao K, Li X. Water transport in polymer electrolyte membrane fuel cells. Prog Energy Combust Sci 2011;37(3):221–91. https://doi.org/10.1016/j.pecs.2010.06.002.

[6] Liu XL, Tao WQ, Li ZY, He YL. Three-dimensional transport model of PEM fuel cell with straight flow channels. J Power Sources 2006;158(1):25–35. https://doi.org/10.1016/j.jpowsour.2005.08.046.

[7] Tao WQ, Min CH, Liu XL, He YL, Yin BH, Jiang W. Parameter sensitivity examination and discussion of PEM fuel cell simulation model validation: Part I. Current status of modeling research and model development. J Power Sources 2006;160(1):359–73. https://doi.org/10.1016/j.jpowsour.2006.01.078.

[8] Wang C, Wang S, Peng L, Zhang J, Shao Z, Huang J, Sun C, Ouyang M, He X. Recent progress on the key materials and components for proton exchange membrane fuel cells in vehicle applications. Energies 2016;9(8):603. https://doi.org/10.3390/en9080603.

[9] Bernardi DM, Verbrugge MW. Mathematical model of a gas diffusion electrode bonded to a polymer electrolyte. AIChE J 1991;37(8):1151–63. https://doi.org/10.1002/aic.690370805.

[10] Bernardi DM, Verbrugge MW. A mathematical model of the solid-polymer-electrolyte fuel cell. J Electrochem Soc 1992;139(9):2477. https://doi.org/10.1149/1.2221251.

[11] Springer TE, Zawodzinski TA, Gottesfeld S. Polymer electrolyte fuel cell model. J Electrochem Soc 1991;138(8):2334. https://doi.org/10.1149/1.2085971.

[12] Nguyen TV, White RE. A water and heat management model for proton-exchange-membrane fuel cells. J Electrochem Soc 1993;140(8):2178. https://doi.org/10.1149/1.2220792.

[13] Min CH, He YL, Liu XL, Yin BH, Jiang W, Tao WQ. Parameter sensitivity examination and discussion of PEM fuel cell simulation model validation: Part II: results of sensitivity analysis and validation of the model. J Power Sources 2006;160(1):374–85. https://doi.org/10.1016/j.jpowsour.2006.01.080.

[14] Fan L, Zhang G, Jiao K. Characteristics of PEMFC operating at high current density with low external humidification. Energy Convers Manag 2017;150:763–74. https://doi.org/10.1016/j.enconman.2017.08.034.

[15] Xia L, Xu Q, He Q, et al. Numerical study of high temperature proton exchange membrane fuel cell (HT-PEMFC) with a focus on rib design. Int J Hydrogen Energy

2021;46(40):21098–111. https://doi.org/10.1016/j.ijhydene.2021.03.192.
[16] Zhang S, Qu Z, Xu H, et al. A numerical study on the performance of PEMFC with wedge-shaped fins in the cathode channel. Int J Hydrogen Energy 2021;46(54):27700–8. https://doi.org/10.1016/j.ijhydene.2021.05.207.
[17] Vijayakrishnan MK, Palaniswamy K, Ramasamy J, et al. Numerical and experimental investigation on 25 cm2 and 100 cm2 PEMFC with novel sinuous flow field for effective water removal and enhanced performance. Int J Hydrogen Energy 2020;45(13):7848–62. https://doi.org/10.1016/j.ijhydene.2019.05.205.
[18] Zhang Z, Liu W, Wang Y. Three dimensional two-phase and non-isothermal numerical simulation of multi-channels PEMFC. Int J Hydrogen Energy 2019;44(1):379–88. https://doi.org/10.1016/j.ijhydene.2018.05.149.
[19] Ebrahimi S, Roshandel R, Vijayaraghavan K. Power density optimization of PEMFC cathode with non-uniform catalyst layer by Simplex method and numerical simulation. Int J Hydrogen Energy 2016;41(47):22260–73. https://doi.org/10.1016/j.ijhydene.2016.07.247.
[20] Atyabi SA, Afshari E. A numerical multiphase CFD simulation for PEMFC with parallel sinusoidal flow fields. J Therm Anal Calorim 2019;135(3):1823–33. https://doi.org/10.1007/s10973-018-7270-3.
[21] Zhao D, Dou M, Zhou D, Gao F. Study of the modeling parameter effects on the polarization characteristics of the PEM fuel cell. Int J Hydrogen Energy 2016;41(47):22316–27. https://doi.org/10.1016/j.ijhydene.2016.09.112.
[22] Wang XD, Xu JL, Lee DJ. Parameter sensitivity examination for a complete three-dimensional, two-phase, non-isothermal model of polymer electrolyte membrane fuel cell. Int J Hydrogen Energy 2012;37(20):15766–77. https://doi.org/10.1016/j.ijhydene.2012.04.029.
[23] Chen H, Liu B, Zhang T, Pei P. Influencing sensitivities of critical operating parameters on PEMFC output performance and gas distribution quality under different electrical load conditions. Appl Energy 2019;255:113849. https://doi.org/10.1016/j.apenergy.2019.113849.
[24] Barati S, Ghazi MM, Khoshandam B. Study of effective parameters for the polarization characterization of PEMFCs sensitivity analysis and numerical simulation. Kor J Chem Eng 2019;36(1):146–56. https://doi.org/10.1016/j.apenergy.2019.113849.
[25] Buckingham E. On physically similar systems; illustrations of the use of dimensional equations. Phys Rev 1914;4(4):345. https://doi.org/10.1103/PhysRev.4.345.
[26] Buckingham E. The principle of similitude. Nature 1915;96(2406):396–7. https://doi.org/10.1038/096396d0.
[27] Mehaeev MA. Fundamentals of heat transfer. Moskva: National Press of Energy; 1956 (In Russian).
[28] De St Q. Issacson E, de St Q. Issacson M. Dimensional methods in engineering and physics. London: Edward Arnold; 1975.
[29] Protsenko VS, Danilov FI. Application of dimensional analysis and similarity theory for simulation of electrode kinetics described by the Marcus–Hush–Chidsey formalism. J Electroanal Chem 2012;669:50–4. https://doi.org/10.1016/j.jelechem.2012.01.028.
[30] Taira H, Liu H. In-situ measurements of GDL effective permeability and under-land cross-flow in a PEM fuel cell. Int J Hydrogen Energy 2012;37:13725–30. https://doi.org/10.1016/j.ijhydene.2012.03.030.
[31] Wang Y, Chen KS. Elucidating two-phase transport in a polymer electrolyte fuel cell, Part 1: characterizing flow regimes with a dimensionless group. Chem Eng Sci 2011;66(15):3557–67. https://doi.org/10.1016/j.ces.2011.04.016.
[32] Koz M, Kandlikar SG. Numerical investigation of interfacial transport resistance due to water droplets in proton exchange membrane fuel cell air channels. J Power Sources 2013;243:946–57. https://doi.org/10.1016/j.jpowsour.2013.06.075.
[33] Cho SC, Wang Y, Chen KS. Droplet dynamics in a polymer electrolyte fuel cell gas flow channel: forces, deformation, and detachment. I: theoretical and numerical analyses. J Power Sources 2012;206:119–28. https://doi.org/10.1016/j.jpowsour.2012.01.057.
[34] Wang Y, Chen KS. Advanced control of liquid water region in diffusion media of polymer electrolyte fuel cells through a dimensionless number. J Power Sources 2016;315:224–35. https://doi.org/10.1016/j.jpowsour.2016.03.045.
[35] Soopee A, Sasmito AP, Shamim T. Water droplet dynamics in a dead-end anode proton exchange membrane fuel cell. Appl Energy 2019;233:300–11. https://doi.org/10.1016/j.apenergy.2018.10.001.
[36] Koz M, Kandlikar SG. Oxygen transport resistance at gas diffusion layer–Air channel interface with film flow of water in a proton exchange membrane fuel cell. J Power Sources 2016;302:331–42. https://doi.org/10.1016/j.jpowsour.2015.10.080.
[37] Koz M, Kandlikar SG. Interfacial oxygen transport resistance in a proton exchange membrane fuel cell air channel with an array of water droplets. Int J Heat Mass Tran 2015;80:180–91. https://doi.org/10.1016/j.ijheatmasstransfer.2014.08.079.
[38] Gyenge EL. Dimensionless numbers and correlating equations for the analysis of the membrane-gas diffusion electrode assembly in polymer electrolyte fuel cells. J Power Sources 2005;152:105–21. https://doi.org/10.1016/j.jpowsour.2005.02.034.
[39] Cho HS, Cho WC, Van Zee JW, Kim CH. A scaling method for correlating ex situ and in situ measurements in PEM fuel cells and electrolyzer. J Electrochem Soc 2018;165(10):F883. https://doi.org/10.1149/2.0041811jes.
[40] Protsenko VS, Danilov FI. Application of dimensional analysis and similarity theory for simulation of electrode kinetics described by the Marcus–Hush–Chidsey formalism. J Electroanal Chem 2012;669:50–4. https://doi.org/10.1016/j.jelechem.2012.01.028.
[41] Iranzo A, Muñoz M, Pino FJ, Rosa F. Non-dimensional analysis of PEM fuel cell phenomena by means of AC impedance measurements. J Power Sources 2011;196(9):4264–9. https://doi.org/10.1016/j.jpowsour.2010.11.004.
[42] Kulikovsky A. Analytical impedance of oxygen transport in a PEM fuel cell channel. J Electrochem Soc 2019;166(4):F306–11. https://doi.org/10.1149/2.0951904jes.
[43] Kulikovsky AA. A physically–based analytical polarization curve of a PEM fuel cell. J Electrochem Soc 2014;161(3):F263–70. https://doi.org/10.1149/2.028403jes.
[44] Kirpichev MV. Theory of similarity. Moskva, SSSR: Press of Academy of Science; 1952 [In Russian)].
[45] Konakov PK. Theory of similarity and its applications in thermal engineering. Leningrad: National Press of Energy; 1959 [In Russian)].
[46] Gurau V, Liu H, Kakac S. Two-dimensional model for proton exchange membrane fuel cells. AIChE J 1998;44(11):2410–22. https://doi.org/10.1002/aic.690441109.
[47] He P, Mu YT, Park JW, Tao WQ. Modeling of the effects of cathode catalyst layer design parameters on performance of polymer electrolyte membrane fuel cell. Appl Energy 2020;277:115555. https://doi.org/10.1016/j.apenergy.2020.115555.
[48] Churchill SW. The Role of analysis in the rate processes. Ind Eng Chem Res 1992;31:643–58. https://doi.org/10.1021/ie00003a002.